JCI insight

Bone marrow is the preferred site of memory CD4$^+$ T cell proliferation during recovery from sepsis

Tomasz Skirecki, … , Dominika Nowis, Ewa Kozłowska

JCI Insight. 2020;5(10):e134475. https://doi.org/10.1172/jci.insight.134475.

Research Article | Immunology | Infectious disease

Graphical abstract

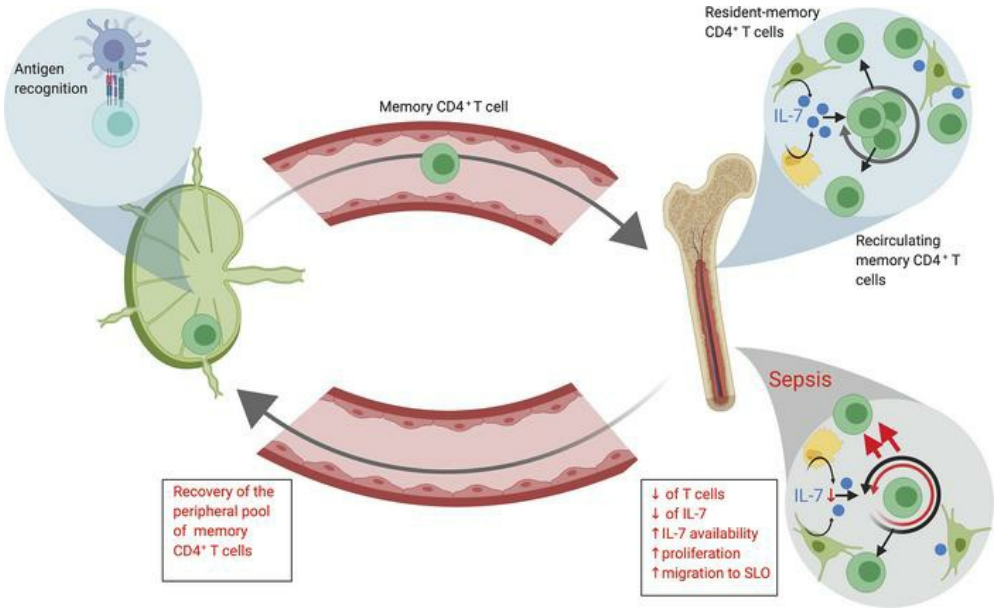

JCI insight

RESEARCH ARTICLE

Bone marrow is the preferred site of memory CD4+ T cell proliferation during recovery from sepsis

Tomasz Skirecki,[1] Patrycja Swacha,[2] Grażyna Hoser,[1] Jakub Golab,[3] Dominika Nowis,[4,5] and Ewa Kozłowska[2]

[1]Laboratory of Flow Cytometry, Centre of Postgraduate Medical Education, Warsaw, Poland. [2]Department of Immunology, Faculty of Biology, University of Warsaw, Warsaw, Poland. [3]Department of Immunology, Medical University of Warsaw, Warsaw, Poland. [4]Laboratory of Experimental Medicine, Centre of New Technologies, University of Warsaw, Warsaw, Poland. [5]Genomic Medicine, Department of General, Transplant and Liver Surgery, Medical University of Warsaw, Warsaw, Poland.

Sepsis survivors suffer from increased vulnerability to infections, and lymphopenia presumably contributes to this problem. The mechanisms of the recovery of memory CD4+ T cells after sepsis remain elusive. We used the cecal ligation and puncture mouse model of sepsis to study the restoration of the memory CD4+ T cells during recovery from sepsis. Then, adoptive transfer of antigen-specific naive CD4+ T cells followed by immunization and BrdU labeling were performed to trace the proliferation and migration of memory CD4+ T cells. We revealed that the bone marrow (BM) is the primary site of CD4+ memory T cell homing and proliferation after sepsis-induced lymphopenia. Of interest, BM CD4+ T cells had a higher basal proliferation rate in comparison with splenic T cells. These cells also show features of resident memory T cells yet have the capacity to migrate outside the BM niche and engraft secondary lymphoid organs. The BM niche also sustains viability and functionality of CD4+ T cells. We also identified IL-7 as the major inducer of proliferation of the BM memory CD4+ T cells and showed that recombinant IL-7 improves the recovery of these cells. Taken together, we provide data on the mechanism and location of memory CD4+ T cell proliferation during recovery from septic lymphopenia, which are of relevance in studying immunostimulatory therapies in sepsis.

Introduction

Because of a high prevalence and unacceptably high mortality, sepsis has been called a global health priority in a World Health Organization resolution (1). Recently, there has been a paradigm shift from defining sepsis as a systemic inflammatory response to infection toward a more complex view underlining a deleterious host response to infection (2). Despite several reports showing trends of decreasing sepsis-associated mortality over recent years (3), other analyses reach less optimistic conclusions (4). Undoubtedly, surviving sepsis negatively affects the long-term health of the patient and increases the risk of later death (5). Among many other negative outcomes, sepsis impairs the immune system, leading to both short- and long-term infectious complications (6). Hence, a better understanding of the pathogenesis of sepsis and its impact on the patient's immune competence are urgently needed.

A key feature of T cells is their functional diversity, e.g., the presence of naive precursors that activate upon specific antigen (Ag) encounter and the possibility of forming a long-lasting but rare memory T cell reservoir. Generation of memory T cells is crucial for rapid and effective defense against a secondary challenge with a specific pathogen. Memory T cells are composed of several subtypes of cells that differ in location, trafficking routes, function, and phenotype. Central memory T cells (Tcm cells) occupy niches in the secondary lymphoid organs (SLOs) and circulate between them, while effector memory T cells (Tem cells) are mostly retained in nonlymphoid tissues (7). A third group composed of tissue-resident memory T cells (Trm cells) represents a generally noncirculating population that settles peripheral tissues (8). Of note, this classification is by no means complete because it lacks other memory phenotypes, such as memory-like T cells, which arise during homeostatic proliferation of naive T cells (9). CD4+ helper T cells play a pivotal role in orchestrating

Conflict of interest: The authors have declared that no conflict of interest exists.

Submitted: October 22, 2019
Accepted: April 9, 2020
Published: May 21, 2020.

Reference information: *JCI Insight*. 2020;5(10):e134475. https://doi.org/10.1172/jci.insight.134475.

the immune response by secretion of cytokines and expression of signaling molecules on their surface (10). Because of their ability to polarize into specific subtypes in a milieu-dependent manner, these cells adapt to support other cells of the immune system, such as macrophages, B cells, $CD8^+$ T cells, and neutrophils, to provide effective protection for the host (11). However, how sepsis affects the compartment of the memory $CD4^+$ T helper cells and how these cells recover after sepsis are currently unexplored.

One of the best recognized features of sepsis-associated immunosuppression is sepsis-induced lymphopenia affecting $CD4^+$ T cells (6, 12). It has been shown that early after the onset of sepsis, in both human patients and in rodent models, a massive lymphocyte apoptosis occurs as a consequence of activation of multiple cell death pathways (13). Lymphopenia was found to be associated with poor prognosis in patients with sepsis (14–16). Importantly, experimental prevention of T cell apoptosis or enhancing recovery by different strategies (caspase inhibitors, IL-7, IL-15, anti–programmed cell death 1) was associated with better outcomes of treated animals and increased resistance to secondary infections (17–20). Most importantly, a first clinical phase I trial with recombinant IL-7 treatment in sepsis has been completed, showing increased recovery of both $CD4^+$ and $CD8^+$ T cells (21). However, the impact of this treatment on memory $CD4^+$ T cells remains unknown (22).

The T cell compartment can be an effective part of adaptive immunity due to the clonal T cell receptor (TCR) diversity and its functional differentiation. Thus, while a numerical recovery of $CD4^+$ T cells in sepsis survivors does certainly take place, only restoration of the presepsis clonal TCR diversity is expected to provide fully efficient adaptive immune protection to patients. Indeed, in septic patients, secondary infections and mortality correlate with strong decline in the TCR diversity and the inability to increase this diversity over time (23). Early murine studies suggested preservation of the TCR clonotypes after the recovery from sepsis (24), but subsequent studies that applied tetramer-based techniques to monitor recovery at the single specific TCR level revealed incomplete numerical recovery of certain clones of naive $CD4^+$ and $CD8^+$ T cells (25–27). Data regarding the functionality of the recovered pathogen-specific T helper cells are contradictory (25, 27), raising doubts about the functionality and relevance of the restored T cell clones in patients with sepsis (22).

Both restoration of T cell numbers and of TCR diversity require T cell proliferation. Most studies on T cells in sepsis investigated changes occurring in the spleen in mice and in the peripheral blood in humans, but the precise site of T cell proliferation after sepsis is still elusive. Thus, even though Cabrera-Perez et al. (25) showed the increase of circulating $CD4^+$ T cells in the active phase of the cell cycle in septic mice, the anatomical location where these cells proliferate remains unknown. This aspect is even more relevant when it comes to memory T cells because these cells exert their function in multiple other tissues and compartments. Interestingly, bone marrow (BM) was found to be an important reservoir of both $CD8^+$ and $CD4^+$ memory T cells in humans and rodents (28–30). Two contradictory models on the role of BM in memory T cell maintenance were proposed, i.e., BM as a temporary niche for proliferation of memory $CD8^+$ T cells and BM as a site for long-term residence and maintenance of memory T cell clones (31). In an attempt to reconcile both concepts, Di Rosa proposed the coexistence of (at least) 2 BM niches for the memory T cells, resembling the organization of hematopoietic stem cell niches (31). Taken together, the existence of the discussed gap in knowledge on the role of BM in maintenance of the Ag-experienced $CD4^+$ T cells led us to investigate it.

This study was designed to characterize the changes in the $CD4^+$ T cell compartment during recovery from sepsis in the SLOs and BM of mice. Our findings support the numerical recovery of circulating T cells. Importantly, we found that the proliferation of memory $CD4^+$ T cells was highest in the BM, which was characterized by the rise in the frequency of $CD69^+$ cells. Adoptive transfer experiments revealed that the BM T cells have a marked predilection to populate the BM niche. By the means of adoptive transfer of OVA-specific $CD4^+$ T cells with subsequent immunization and cecal ligation and puncture (CLP), we showed that bona fide memory helper T cells indeed proliferate and expand in the BM during the recovery phase of sepsis in an IL-7–dependent mechanism, and then a fraction of these cells migrates to the periphery.

Results

Sepsis-induced changes in T cell populations. CLP is a commonly used model of resuscitated septic peritonitis (32) that reproduces immune-inflammatory responses affecting human patients during sepsis. Specifically, a mild model of low-lethality CLP was performed to create homogenous response in septic animals and to gain the opportunity of studying the recovery phase of the disease (Supplemental Figure 1A; supplemental material available online with this article; https://doi.org/10.1172/jci.insight.134475DS1). Mice showed clinical features of sepsis, including hypothermia, hunched position, piloerection, and diarrhea. In contrast to most murine studies, which focus on the splenic T cell compartment, we took advantage of the

low-volume sampling method to analyze the numerical changes of T cells in the peripheral blood of septic animals. As expected, CLP induced a profound lymphopenia in 48 hours, with subsequent recovery of T cell numbers that was complete 7 days post-CLP (Supplemental Figure 1, B–D). We therefore decided to study T cell proliferation before complete recovery, i.e., on day 6 after CLP.

Sepsis affects the frequency and phenotype of CD4$^+$ T cells. To further characterize sepsis-induced changes in CD4$^+$ T cells, we analyzed the phenotype of these cells in the lymph nodes, spleen, and BM. Sepsis led to a marked reduction in CD4$^+$ T cell counts 7 days post-CLP in all investigated organs (Figure 1, A–D), which was sustained for 14 days except in the lymph nodes (Figure 1, B–D). We also characterized the impact of sepsis on the phenotypes of the CD4$^+$ T cells using commonly used markers for identification of naive and memory T cells (33). As expected, sepsis led to a transient increase in the frequency of the effector CD44$^-$ CD62L$^-$ T cells in the lymph nodes (Figure 1B) and spleen (Figure 1C), accompanied by a decrease in the percentage of naive CD44$^-$CD62L$^+$ CD4$^+$ T cells in SLOs (Figure 1, B and C). Additionally, the subpopulation of effector memory–phenotype CD44$^+$CD62L$^-$ T cells in the spleen steeply dropped from the mean of 12.7% in control mice to 4.7% on day 7 after CLP to 0.05% 14 days after the septic insult (Figure 1C). A similar pattern was observed for the central memory CD44$^+$CD62L$^+$ T cells (Figure 1C). Interestingly, quite different dynamics were observed in the BM. The subpopulation of Tem cells, which constitutes the main subpopulation of CD4$^+$ cells in the BM of healthy mice, expanded significantly after CLP from 51.2% to 66.3% 7 days after CLP and up to 81.2% 14 days after CLP (Figure 1D). Altogether, these observations support the sepsis-associated loss of CD4$^+$ T cells in the periphery and indicate a discrete accumulation and the expansion of effector lymphocytes in the SLOs. Importantly, our data indicate that the BM is a site that preserves the memory CD4$^+$ T cells after septic insult.

BM maintains proliferation of effector memory–phenotype CD4$^+$ T cells in postseptic mice. As already stated, we hypothesized that the robust proliferation of CD4$^+$ T cells takes place around day 7 after the onset of sepsis. Therefore, to characterize the proliferation of T cells, we administered a bolus of BrdU on either day 6 or 13 after CLP and analyzed the rate of proliferating T cells 24 hours later at different sites (Figure 2A). In control mice, there were no differences in the percentage of BrdU-incorporating CD4$^+$ T cells among analyzed organs (Figure 2, B and C). However, in sepsis survivors 7 days after CLP, there was a significant increase in actively proliferating CD4$^+$ T cells in the BM (by 4-fold), whereas neither splenic nor lymph node T cells increased their proliferation rate (Figure 2C). At the later investigated time point (14 days post-CLP), the proliferation rates in all organs returned to the levels observed in the control mice (Figure 2C). Subsequent analysis of subset composition of the proliferating fraction of CD4$^+$ T cells revealed that the Tem cells constituted the largest subpopulation of proliferating cells in the lymph nodes, spleen, and BM (Figure 2D). Sepsis survivors showed an increased proportion of actively cycling naive CD4$^+$ T cells in the lymph nodes (20.3% in controls vs. 72% 14 days post-CLP, $P < 0.01$; Figure 2D), while in the spleen the majority of cycling cells were the effector CD4$^+$ T cells: 4.4% in controls vs. 61.1% vs. 66.7% on day 7 ($P < 0.05$) and day 14 ($P < 0.01$) after CLP, respectively (Figure 2D). In line with the reduction of the frequency of memory phenotype T cells in the spleen, the frequency of proliferating memory phenotype CD4$^+$ T cells was also severely diminished by the septic insult (Figure 2D). Notably, no significant shift occurred in the ratio of the proliferating T cell subsets in the BM, with CD4$^+$ Tem cells representing the predominant fraction (Figure 2D). Altogether, these data show that BM is a privileged site of the effector memory–phenotype CD4$^+$ T cell proliferation during recovery from sepsis.

Sepsis does not affect compartment-specific features of the CD4$^+$ T cells in the BM. Previously, both human and murine BM T cells were found to express high levels of CD69 (29, 34), a type II membrane receptor, which appears on the cell surface upon TCR activation and facilitates BM homing of memory T cells (34). Therefore, we aimed to assess whether sepsis affects the expression of CD69 on BM CD4$^+$ T cells. As expected, in control mice, only CD4$^+$ T cells from the BM had a substantial fraction of CD69$^+$ cells (Figure 3, A, and B). Sepsis induced transient expression of CD69 in the effector T cells in the spleen, which supports previous observations (35), but not in the lymph node T cells (Figure 3, A–C). In the BM, there was a further increase in the frequency of CD69$^+$CD4$^+$ T cells reaching 4-fold upregulation on day 14 after CLP, which was the period of observation (Figure 3B). Invariably, in the BM, CD69 was expressed mostly by the Tem cells (Figure 3C), reflecting their increase in sepsis survivors (Figure 2D). Because CD69 is also regarded as a marker of the Trm cells, we asked whether the cells that we had analyzed were separated from the microcirculation of the BM. For this purpose, we used the technique of in vivo antibody staining (36) in mice recovering from sepsis on day 7. In septic mice, more than 98% of proliferating memory CD4$^+$ T cells in the BM were separated from

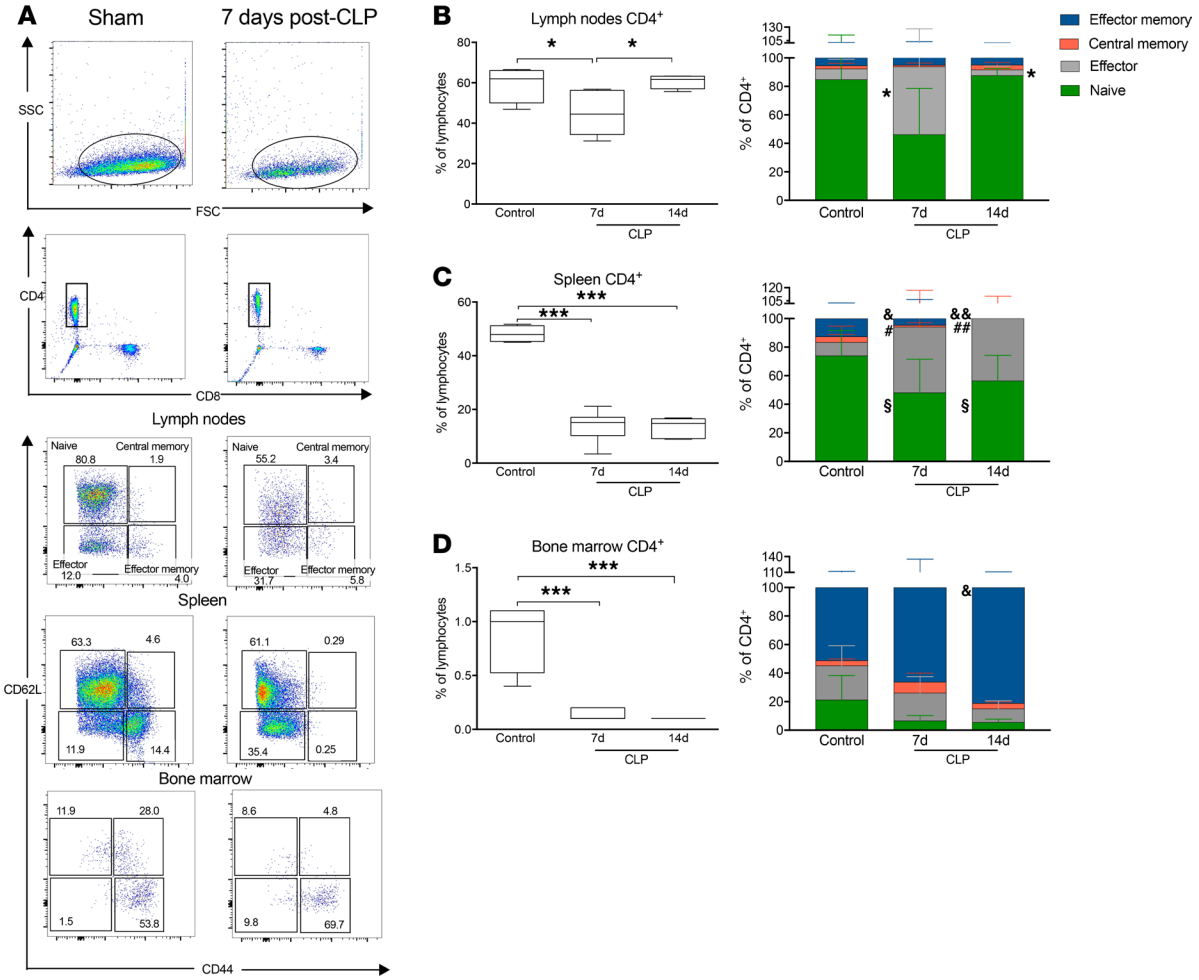

Figure 1. Sepsis induces changes in CD4⁺ T cell subsets' frequency. (**A**) Representative flow cytometry plots showing CD4⁺ T cell gating strategy used for the analysis of naive ($CD44^-CD62L^+$), central memory ($CD44^+CD62L^+$), effector memory ($CD44^+CD62L^-$), and effector ($CD44^-CD62L^-$) CD4⁺ T cells. (**B**) Changes in the frequencies of CD4⁺ T cells in the lymph nodes after sepsis (left), with shifts in subset composition of the CD4⁺ T cells after sepsis (right graph). (**C**) Changes in the frequencies of CD4⁺ T cells in the spleen after sepsis (left), with shifts in subset composition of the CD4⁺ T cells after sepsis (right graph). (**D**) Changes in the frequencies of CD4⁺ T cells in the BM after sepsis (left), with shifts in subset composition of the CD4⁺ T cells after sepsis (right graph). Box-and-whiskers plots present 25th through 75th percentiles (p25-p75) (box), mean, and p10-p90 (whiskers). Data from 2 independent experiments (n = 6–8 in each group). *$P < 0.05$, and ***$P < 0.001$ using ANOVA with Tukey's post hoc test. Superimposed graphs: sign on the left side of bar represents $P < 0.05$ between day 7 and controls; sign on the right side of bar represents $P < 0.05$ between days 14 and 7. "*" represents differences between effector; "&" effector memory; "#" central memory; and "§" naive CD4⁺ T cells at different time points using ANOVA with Tukey's post hoc test.

the peripheral blood, showing their distinctive features (Supplemental Figure 2). Interestingly, in contrast to splenic T cells, the BM-resident CD4⁺ T cells were protected from apoptosis (Supplemental Figure 3). Moreover, the subpopulation of IFN-γ–producing $CD4^+CD44^+$ T cells was 2-fold higher in the BM in comparison with the spleen (Supplemental Figure 4). Importantly, 7 days after CLP the frequencies of IFN-γ–, IL-4–, and IL-17A–producing memory CD4⁺ T cells remained unaltered in the BM while the subpopulations of splenic IFN-γ^+ and IL-4^+ CD4⁺ T cells were decreased (Supplemental Figure 4). Altogether, these data imply that the effector memory–phenotype CD4⁺ cells in the BM have features of Trm cells.

Ag-specific CD4⁺ Tem cells proliferate in the BM during recovery from sepsis. Specific pathogen–free lab mice develop mainly naturally occurring memory phenotype CD4⁺ T cells, which differ from the Ag-specific memory T cells in terms of proliferation requirements (9). Therefore, to verify that during recovery from sepsis BM supports the proliferation of the "true" Ag-experienced memory T cells, we designed an immunization experiment with TCR-specific T cells. For this purpose, we performed adoptive transfer of OVA-specific naive $CD4^+CD44^-$ cells from B6.Cg-Tg(TcraTcrb)425Cbn/J (OT-II) mice into naive WT C57BL/6 mice as described in Methods (Figure 4A). Then, mice were immunized with OVA and 30 days later subjected to CLP. The transferred cells became CD44⁺, confirming induction of the memory

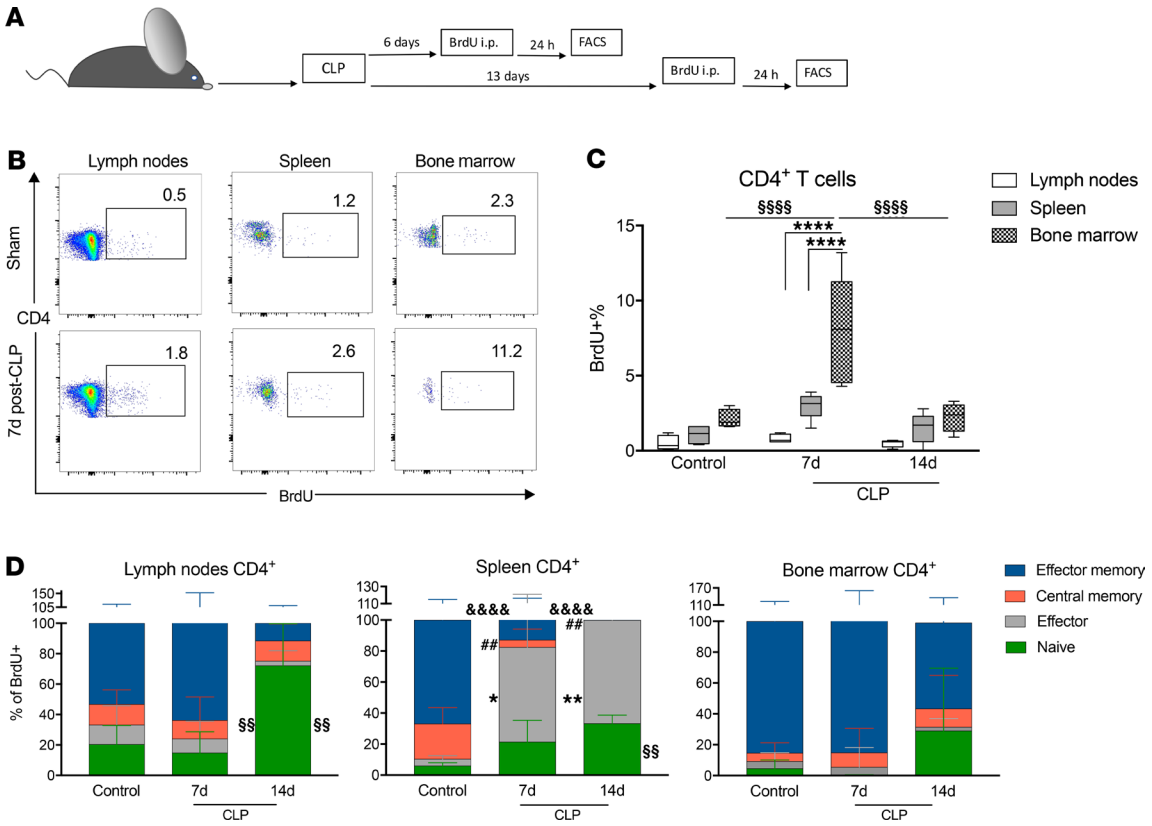

Figure 2. BM contains actively proliferating CD4⁺ T cells after sepsis. (**A**) Experimental design. Mice underwent CLP surgery and subsequent treatment with antibiotic and fluid resuscitation. On day 6 or 13 after surgery, mice were injected with a bolus of BrdU i.p. Twenty-four hours later the cells were isolated from organs and analyzed by flow cytometry. (**B**) Representative flow cytometry plots showing CD4⁺BrdU⁺ cells that were actively cycling after BrdU administration. Upper row shows plots from sham animals, and lower row shows plots from 7 days post-CLP mice. (**C**) Percentage of BrdU⁺ cells among CD4⁺ T cells from different organs at given time points after CLP (n = 6–8 in each group); box-and-whiskers plot presents p25-p75 (box), mean, and p10-p90 (whiskers). ****P < 0.0001 between BM and lymph nodes or spleen; §§§§P < 0.0001 between BM 7 days after CLP and control or 14 days post-CLP using ANOVA with Tukey's multiple-comparisons test. (**D**) Changes in the subset composition of CD4⁺ T cells that incorporated BrdU. Data from 2 independent experiments are shown (n = 6–8). Superimposed graphs: sign on the left side of bar represents P < 0.05 between day 7 and control; sign on the right side of bar represents P < 0.05 between days 14 and 7. "*" represents differences between effector; "&" effector memory; "#" central memory; and "§" naive CD4⁺ T cells at different time points using ANOVA with Tukey's post hoc test.

phenotype (Supplemental Figure 5). On the sixth day post-CLP mice were injected with the BrdU bolus. Enrichment of the OT-II CD4⁺ T cells with the specific tetramer enabled us to perform reliable analysis of the rare cells (Figure 4, B and C). On day 7 after CLP, BM was a major site of the proliferation of memory CD4⁺ OT-II cells both in absolute values and percentage of BrdU⁺ cells (Figure 4, D and E). As shown in Figure 4F, BM contained a 7-fold greater number of proliferating OT-II cells compared with lymph nodes or spleen. Sham animals transferred with OT-II cells and immunized with OVA had a higher frequency of proliferating CD4⁺ memory T cells in the BM, but it was not reflected by the absolute number of proliferating cells (Figure 4, D and E). We took advantage of the short in vivo half-life of BrdU (37) and used single-pulse BrdU labeling to trace the T cells that had proliferated on the sixth day post-CLP. Based on the findings by other groups, it was assumed that the fraction of the cells that had incorporated BrdU was relatively stable and should not complete more than 3 divisions before the end of the experiment (38–40). This helped us unravel that 36 days after CLP, most of the cells that had incorporated BrdU during day 6 post-CLP were found in the lymph nodes (Figure 4D). However, when we looked at the frequencies of BrdU⁺ cells, it turned out that among the BM-resident OT-II CD4⁺ T cells, the BrdU⁺ cells constituted 6.7% while in lymph nodes or spleen their frequency was as low as 0.5%, which suggests preferential retention of the postmitotic T cells in the BM. Additionally, we performed a similar experiment using BALB/c and syngeneic OVA-specific TCR DO10.11 mice, which confirmed the findings in B6/OT-II mice (Supplemental Figure 6). Taken together, these results show that the Ag-experienced memory CD4⁺ T cells proliferate extensively during the resolution of sepsis and later they

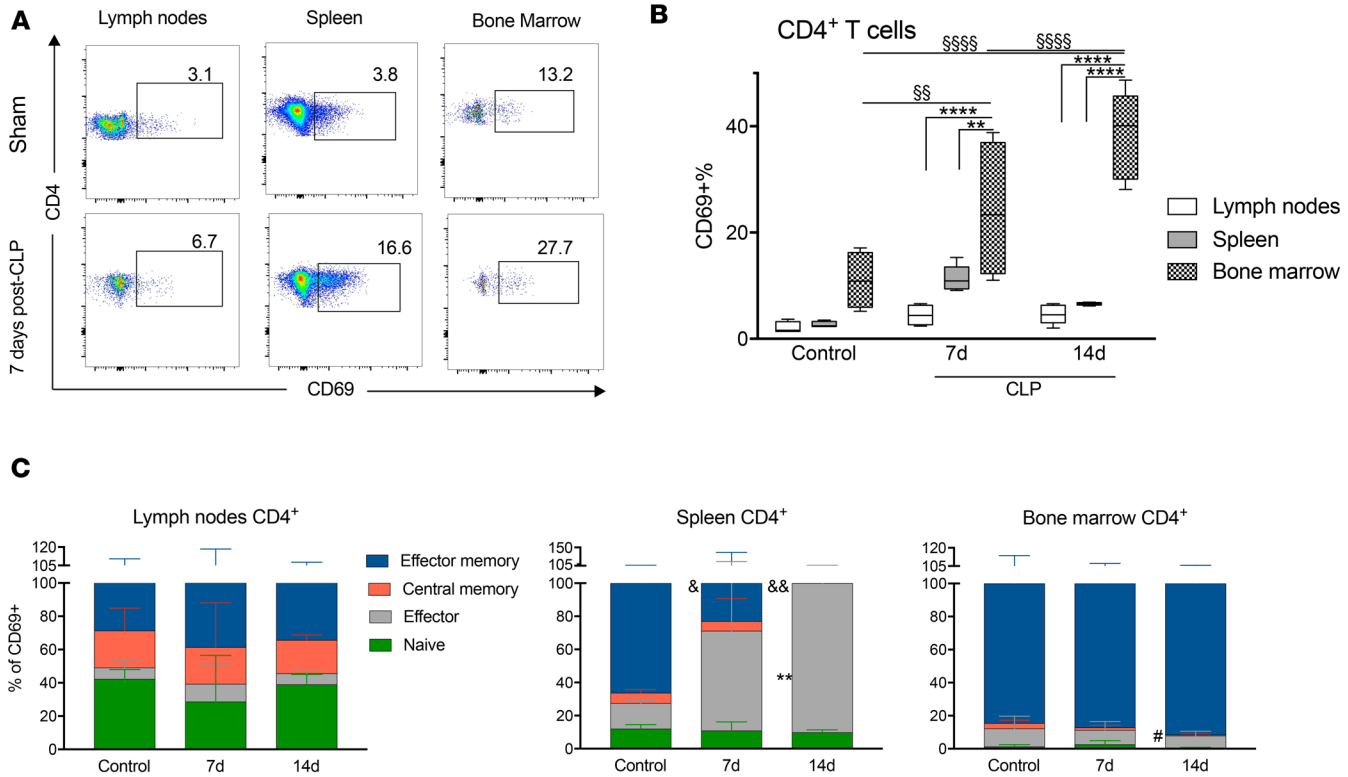

Figure 3. Sepsis leads to accumulation of CD69⁺ T cells in the BM. (**A**) Representative flow cytometry plots showing expression of CD69 on CD4⁺ cells from lymph nodes, spleen, and BM of sham (upper row) and septic (lower row) mice. (**B**) Percentage of CD69⁺ cells among CD4⁺ T cells from different organs at given time points after CLP (n = 6–8 in each group). Box-and-whiskers plot presents p25-p75 (box), mean, and p10-p90 (whiskers). $^{**}P < 0.01$, and $^{****}P < 0.0001$ between BM and lymph nodes or spleen; §§$P < 0.01$ between control BM and 7 days after CLP; and §§§§$P < 0.0001$ between BM 14 days after CLP and control or 7 days post-CLP using ANOVA with Tukey's multiple-comparisons test. (**C**) Changes in the composition of CD4⁺ T cell subsets expressing CD69 after CLP sepsis. Data from 2 independent experiments are shown (n = 6–8 in each group). Superimposed graphs: sign on the left side of bar represents $P < 0.05$ between day 7 and control; sign on the right side of bar represents $P < 0.05$ between days 14 and 7. "*" represents differences between effector; "&" effector memory; "#" central memory; and "§" naive CD4⁺ T cells at different time points using ANOVA with Tukey's post hoc test.

migrate out of the BM to replenish the lost cells at other anatomical locations. At the same time, a small population of these extensively proliferating CD4⁺ cells persist in the BM.

BM T cell–specific niche is compromised in sepsis. It has been postulated that BM creates niches for the memory T cells that are composed of myeloid and stromal cells producing IL-7, IL-15, and collagen (28, 30). We asked whether sepsis modulates the specificity and capacity of these niches. To address this question, we performed adoptive transfer experiments with T cells isolated from healthy or postseptic BALB/c mice and transplanted them into either healthy or post-CLP recipient mice (Figure 5A). We transplanted relatively low numbers of T cells to avoid their excessive nonspecific accumulation and to trace their homing in recipients that were not severely lymphopenic. Analysis of the donor cells was performed 7 days after the transfer to let the cells equilibrate between the preferred niches. In healthy mice, T cells isolated from the spleen of normal mice homed very poorly to the BM (Figure 5B). In contrast, T cells isolated from normal BM efficiently engrafted the BM of a healthy host (Figure 5C). However, when T cells were transplanted into a postseptic host, the homing of BM T cells in the host's BM was significantly impaired (Figure 5C). This was also true for the T cells from a septic donor. Interestingly, the homing capacity of lymph nodes for splenic T cells increased after sepsis but decreased for the BM T cells (Figure 5, B and C). In sum, these data imply that the BM-resident T cells have homing specificity toward the BM, but the capacity of this niche decreases in sepsis.

BM IL-7 supports proliferation of CD4⁺ T cells during recovery from sepsis. Because the BM CD4⁺ T cells were previously found in close proximity to IL-7–producing cells (30) and IL-7 treatment was shown to enhance T cell recovery after sepsis (17, 21), we hypothesized that this cytokine might be critical for the observed T cell proliferation in the BM after sepsis. To test this possibility, we first analyzed the IL-7 levels after sepsis in the plasma and the BM. We detected relatively high concentrations of IL-7 in the BM of healthy mice, which

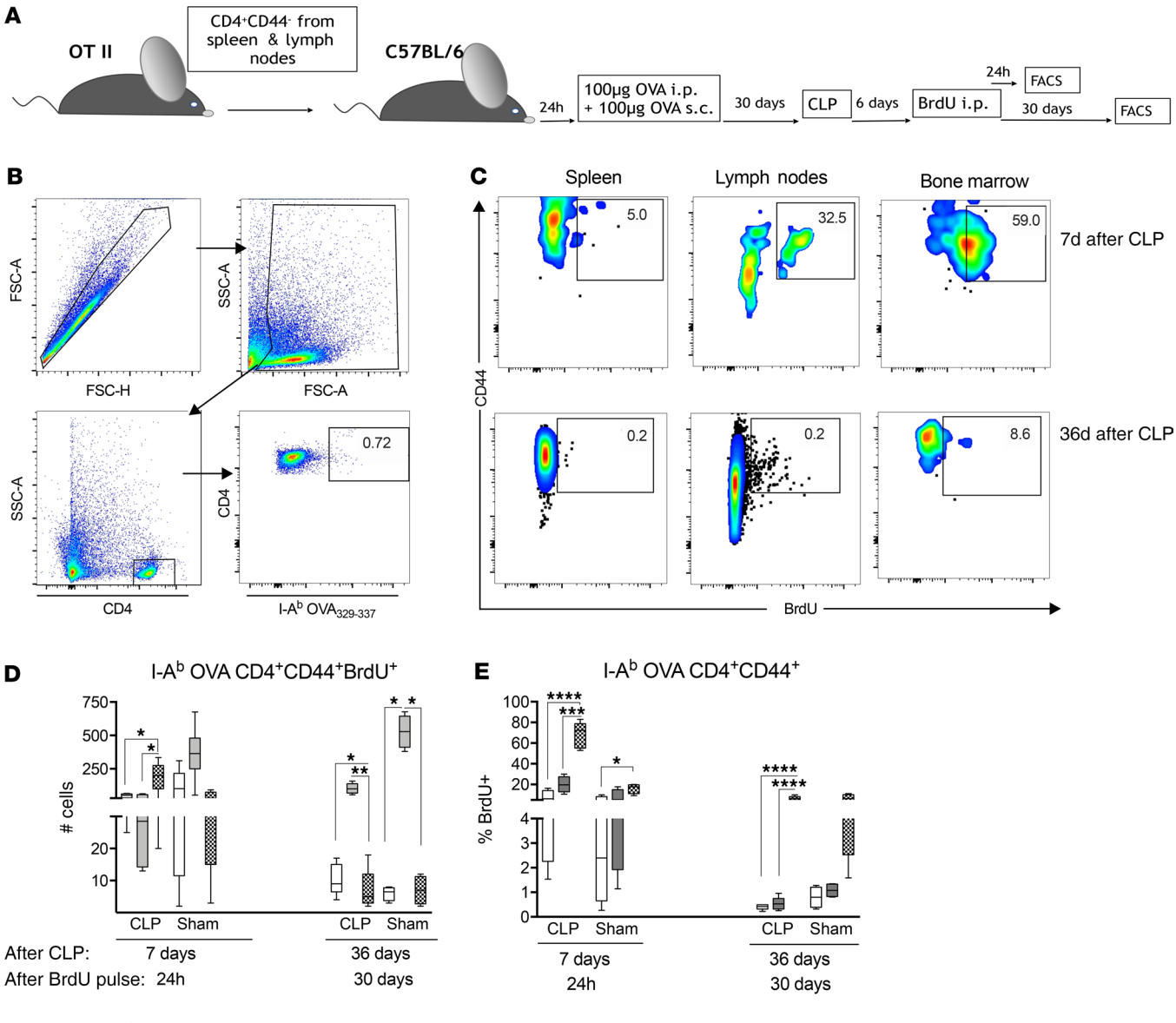

Figure 4. BM supports proliferation of specific Ag-experienced memory CD4⁺ T cells in sepsis. (**A**) Experimental design. CD4⁺CD44⁻ naive T cells were isolated from young OT-II mice and transferred to C57BL/6 recipients. Then, mice were immunized with 100 µg of OVA i.p. and 100 µg s.c. Thirty days later mice were subjected to CLP and received a bolus of BrdU on day 6 after surgery. Cells were analyzed 24 hours or 30 days later by flow cytometry. (**B**) Plots showing flow cytometry gating strategy of the transplanted I-A^b OVA$_{329-337}$ tetramer-specific CD4⁺ T cells after nanobead enrichment. (**C**) Representative flow cytometry plots showing analysis of BrdU⁺ cells that are CD4⁺I-A^b OVA$_{329-337}$⁺CD44⁺ from mice that had CLP surgery 7 days (upper row) and 36 days (lower row) before. (**D**) Total number of the I-A^b OVA CD4⁺BrdU⁺ cells in lymph nodes, spleen, and BM of mice post-CLP and sham mice at different times after BrdU injection. (**E**) Percentage of BrdU⁺ cells among the I-A^b OVA CD4⁺ cells in lymph nodes, spleen, and BM of mice post-CLP and sham mice at different times after BrdU injection. (**F**) Normalized ratios of the number of I-A^b OVA CD4⁺BrdU⁺ cells in the lymph nodes and BM versus the number of I-A^b OVA⁺CD4⁺BrdU⁺ in the spleen. Box-and-whiskers plot presents p25-p75 (box), mean, and p10-p90 (whiskers). Results from the mice post-CLP and sham mice at different times after BrdU injection. Data from 2 independent experiments (n = 6–10 in each group). *P < 0.05, **P < 0.01, ***P < 0.001, and ****P < 0.0001 using ANOVA with Tukey's post hoc test.

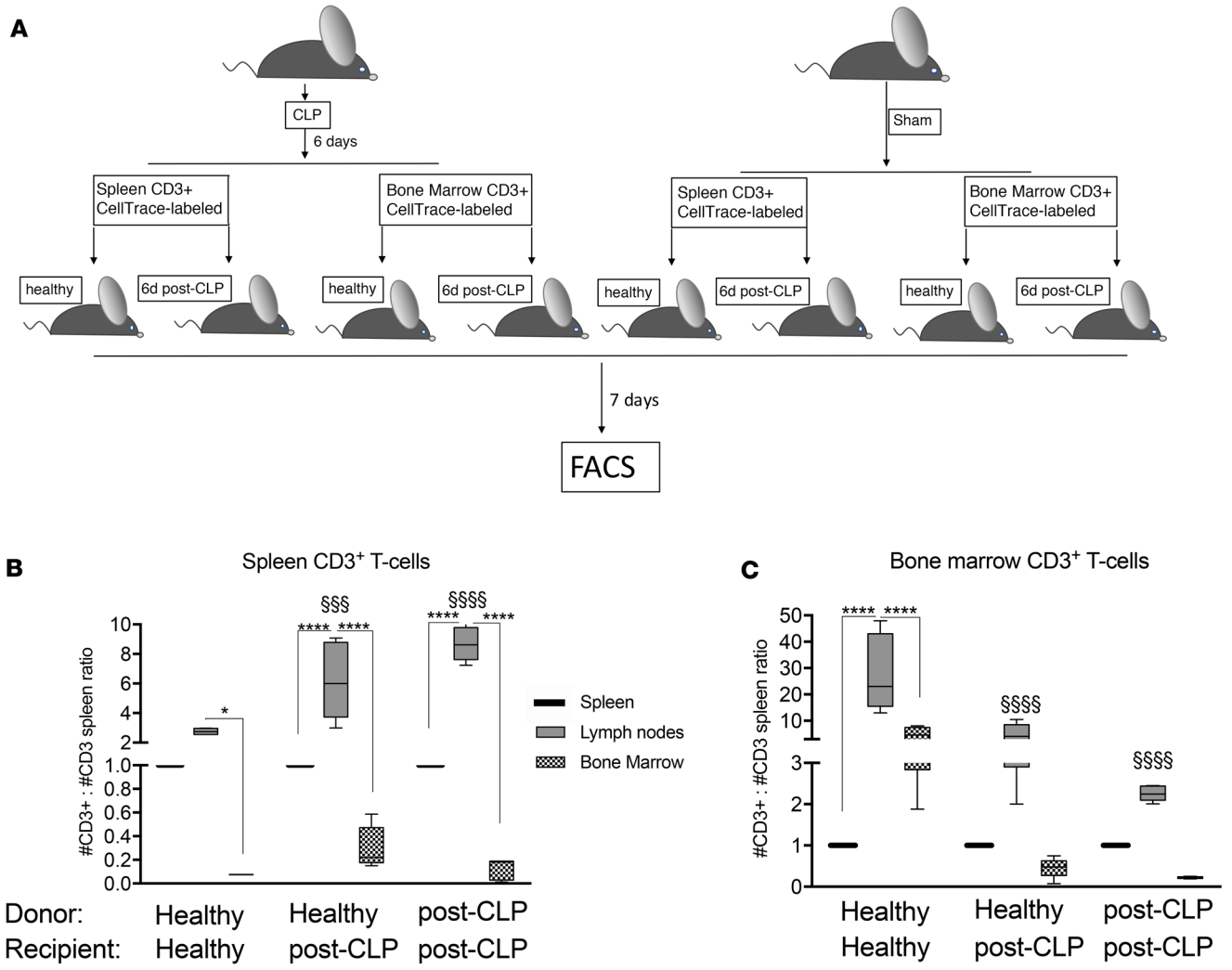

Figure 5. The capacity of T cell homing toward the BM niche is decreased in sepsis. (**A**) Experimental design. CD3⁺ T cells were purified from healthy or post-CLP mice on day 6. Then cells were labeled with CTV and transplanted into healthy or post-CLP mice (on day 6). Twenty-four hours later fluorescently labeled cells were analyzed by flow cytometry. (**B**) Normalized ratio of the number of donor-origin splenic T cells in the lymph nodes or BM of recipient mice versus the number of donor-origin cells in the spleen (n = 5–8 in each group). (**C**) Normalized ratio of the number of donor-origin BM T cells in the lymph nodes or BM of recipient mice versus the number of donor-origin cells in the spleen. Box-and-whiskers plot presents p25-p75 (box), mean, and p10-p90 (whiskers). Data from 2 independent experiments (n = 5–8 in each group). *$P < 0.05$, ****$P < 0.0001$, §§§$P < 0.001$, and §§§§$P < 0.0001$ for differences between CD3 ratio in the lymph nodes of healthy-healthy and other combinations using ANOVA with Tukey's post hoc test.

were decreasing after sepsis for the whole observation period of 14 days (Figure 6A). At the same time, the serum concentration of IL-7, which was low in the healthy mice, peaked 72 hours post-CLP, went low on day 7, and began to rise on day 14 (Figure 6A). Such complex kinetics could reflect and rationalize previous discrepancies in human studies (41, 42). Nevertheless, IL-7 exerts its function in T cell biology via its extracellular matrix–bound form (9). We analyzed its availability in situ in the BM after CLP sepsis. Confocal microscopy observations of the bone sections confirmed the findings of the reduced but preserved production of IL-7 in the BM (Figure 6B). Then, we asked whether this reduced concentration of IL-7 is responsible for stimulation of T cell proliferation in the BM. Blockade of the IL-7R for 2 consecutive days starting from day 5 after CLP significantly reduced the rate of cell cycling in the BM CD4⁺ T cells to a level only slightly higher than in control mice ($P > 0.05$) (Figure 6C). Taken together, sepsis downregulates IL-7 level in the BM niche, but the residual level of this cytokine sufficiently drives the proliferation of memory CD4⁺ T cells.

Exogenous recombinant IL-7 enhances proliferation of BM memory CD4⁺ T cells. Because we found that the recovery of BM CD4⁺ T cells depends on the local IL-7 availability, we tested whether this process can be enhanced by treatment with exogenous IL-7 (Figure 7A). Treatment with rm-IL-7 increased the prolifera-

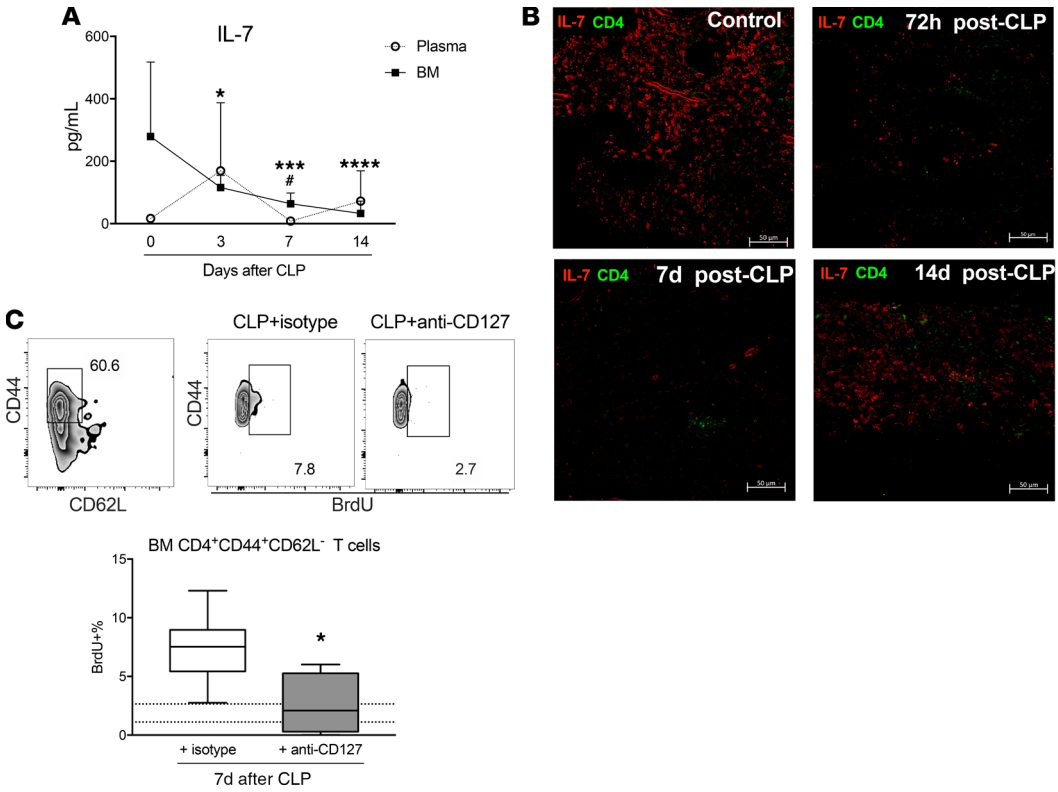

Figure 6. IL-7 drives proliferation of CD4⁺CD44⁺CD62L⁻ T cells in the BM after sepsis. (**A**) Kinetics of IL-7 levels in the plasma and BM after sepsis. IL-7 concentration was measured in the sera and BM supernatants of healthy and postseptic mice at different time points (n = 6–8). For plasma: $^{\#}P < 0.05$ between 72 hours and 7 days. For BM: $^{*}P < 0.05$, $^{***}P < 0.001$, and $^{****}P < 0.0001$ using ANOVA multiple-comparisons with Tukey's post hoc test. (**B**) Confocal microscopy photographs of the BM sections show IL-7 (red) and CD4⁺ T cells (green) (representative of n = 4). Scale bar: 50 μm. (**C**) IL-7 is responsible for the proliferation of CD4⁺CD44⁺CD62L⁻ T cells after sepsis. Post-CLP mice received anti–IL-7R (anti-CD127) antibody on days 5 and 6 of sepsis and a bolus of BrdU on day 6. BrdU incorporation was evaluated by FACS 24 hours later. Representative plots are shown. Box-and-whiskers plot presents p25-p75 (box), mean, and p10-p90 (whiskers). Dashed line shows range of BrdU⁺CD4⁺CD44⁺CD62L⁻ cells in control mice. $^{*}P < 0.05$ (n = 6 per group) using Student's t test.

tion rate of CD4⁺ T cells in the spleen and BM but not in the lymph nodes (Figure 7, B–D). The increase in the cycling CD44⁺ T cells was observed only in the BM, and it was followed by their enhanced numerical recovery. Although the treatment with rm-IL-7 did not affect the percentages of BrdU-incorporating T cells in the lymph nodes, it enhanced the numerical recovery of CD4⁺ T cells.

Discussion

Impaired immunity and susceptibility to infections are among the most critical problems in sepsis survivors (43). CD4⁺ memory T cells constitute a key part of the immune memory system, enabling rapid expansion and cytokine production upon secondary Ag encounter. However, sepsis induces massive attrition of memory CD4⁺ T cells throughout the body. Understanding of the mechanisms regulating recovery of the CD4⁺ memory T cells in sepsis patients is crucial for the successful development of immunomodulating therapies. Therefore, we performed this study to characterize the recovery of CD4⁺ memory T cells after sepsis, with a special focus on identifying the anatomical sites of T cell expansion. Our results indicate that BM is a privileged site of the effector memory CD4⁺ T cell proliferation in sepsis and also under physiological conditions. Although the capacity of the BM niche is diminished in sepsis, this organ is still able to support the viability, functionality, and proliferation of memory CD4⁺ T cells in an IL-7–dependent manner. Moreover, for the first time to our knowledge, we show that the BM niche governs proliferation of Ag-specific memory CD4⁺ T cells after sepsis.

Recovery from sepsis-induced lymphopenia was shown to correlate with survival and presumably is related to long-term morbidity and health of the survivors (14). Our early experiments showed rapid numerical recovery of both CD4⁺ and CD8⁺ T cells in septic mice. There are 2 mechanisms that can cooperate to restore T cell counts, i.e., de novo thymopoiesis and peripheral homeostatic proliferation. So far, relatively

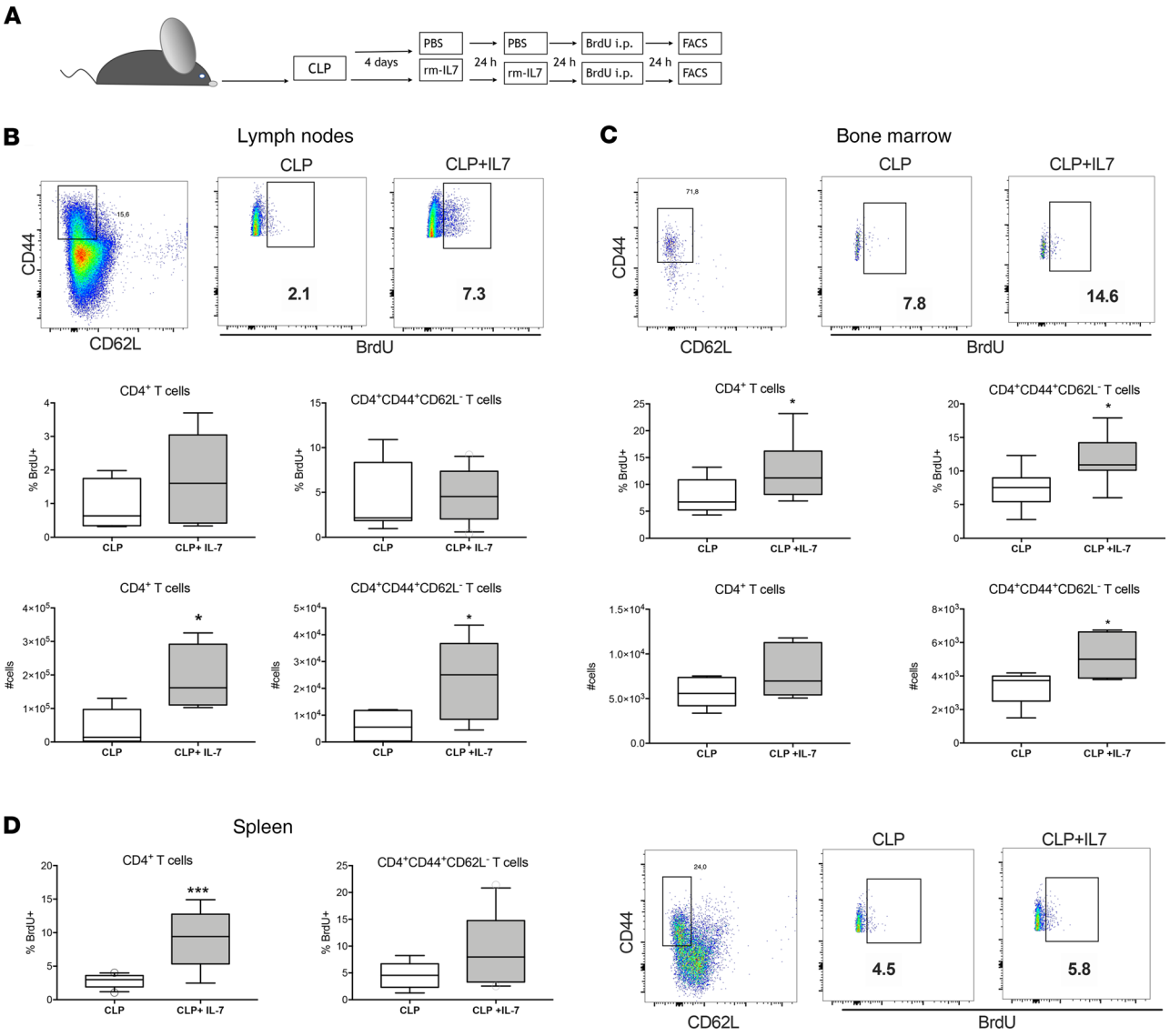

Figure 7. Exogenous IL-7 increases proliferation of CD4⁺ T cells including BM CD4⁺CD44⁺ T cells. (**A**) Experimental design. On days 4 and 5 after CLP, mice were given 2 injections of recombinant murine IL-7 (rm-IL-7) s.c. and on day 6 a bolus of BrdU i.p. 24 hours later. Cell numbers and proliferation rates were analyzed by flow cytometry. (**B**) Representative dot plots and frequencies of BrdU-incorporating T cells from the lymph nodes are shown. Absolute counts of $CD4^+$ and $CD4^+CD44^+CD62L^-$ T cells from 2 axillary and 2 popliteal lymph nodes are shown. (**C**) Representative dot plots and frequencies of BrdU-incorporating cells from the BM are shown. Absolute counts of $CD4^+$ and $CD4^+CD44^+CD62L^-$ T cells from 2 femurs are shown. (**D**) Representative dot plots and frequencies of BrdU-incorporating cells from the spleen are shown. Box-and-whiskers plots present p25-p75 (box), mean, and p10-p90 (whiskers). Data from 2 independent experiments ($n = 10$ in each group). $^*P < 0.05$, and $^{***}P < 0.001$ using Student's t test.

little is known about these processes in sepsis. It could be anticipated that thymopoiesis is not a relevant process in human patients in the postsepsis T cell recovery because (a) this process is not very active in adult humans (44); (b) thymic output is poorly regulated by peripheral lymphopenia (45); and (c) septic mice present dysfunctional thymopoiesis (46, 47). Importantly, thymopoiesis would not be able to recover memory T cells. However, in their pioneering work on the topic, Richard Hotchkiss's group postulated that in contrast to $CD8^+$ T cells, $CD4^+$ T cells do not undergo homeostatic proliferation in sepsis survivors (24). This conclusion was drawn upon the analysis of proliferation of transplanted OT-II cells in the spleens of recipient mice (24). It has been proposed that the extremely high number of transferred cells might not recapitulate physiological response (25). Also, the proliferation of the transferred cells was not investigated in organs other than the spleen (24). In contrast, follow-up studies suggested homeostatic proliferation to be a process responsible for the restoration of the peripheral $CD4^+$ T cell pool (25, 27). It must be emphasized

that these studies focused on naive $CD4^+$ T cells while sepsis induces attrition of both naive and memory $CD4^+$ T cell pools to a similar rate (48). Due to complete lack of knowledge on the restoration of $CD4^+$ T cells in sepsis, in this study we focused particularly on this cell type and therefore decided to analyze their proliferation rate not only in the spleen but also in lymph nodes and BM, which host Tcm cells and Tem cells, respectively. Interestingly, we observed increased frequency of effector $CD4^+$ T cells in SLOs with a concomitant decrease of $CD44^+CD4^+$ T cells, which stays in contrast with previous observations (24). However, we observed that in the BM the $CD4^+$ Tem cells remained the main $CD4^+$ subpopulation and expanded over time after CLP sepsis. Although there was an increase in the percentage of proliferating $CD4^+$ T cells in SLOs on day 7 after sepsis, these rates were relatively low and much lower in comparison with those in the BM. Thus, we conclude that the homeostatic proliferation of memory $CD4^+$ T cells occurs in the BM. Although BM was already shown to harbor a pool of memory $CD4^+$ T cells, the data on their proliferation are scarce, especially in comparison with $CD8^+$ cells (31). Murine studies revealed a low rate of actively cycling $CD4^+$ cells in the BM (30), while a high basal proliferation rate was found in nonhuman primates and was further enhanced after T cell depletion (49). Our results clearly indicate that BM is also a niche for the proliferation of memory $CD4^+$ T cells during recovery from sepsis. The BM niche is also unique because it preserves viability and ability to produce cytokines by the memory $CD4^+$ T cells. BM $CD4^+$ T cells express high levels of CD69 receptor, which is probably responsible for their homing and endurance at that site by inhibition of the sphingosine-1-phosphate receptor (S1PR1) (34). We observed that sepsis further increases the frequency of $CD69^+$ Tem cells in the BM, which might be the effect of their selective homing. However, increased homing could be the consequence of reduced serum concentration of sphingosine-1-phosphate in sepsis (50), which would rather suggest that inhibition of S1PR1 by CD69 is not critical. Another explanation for the accumulation of $CD69^+CD4^+$ T cells in the BM could be in situ activation because circulating dendritic cells can deliver Ags to the BM T cells (51), albeit a similar increase in CD69 expression was not seen in SLOs.

The adult human T cell pool is composed mainly of memory T cells, and almost all organs contain mature and differentiated Trm cells (52, 53). Clearly, mice housed under the specific pathogen–free (SPF) conditions have mainly naive T cells that can eventually become memory phenotype cells after undergoing homeostatic proliferation (54). Also, these animals are poorly seeded by populations of differentiated Trm cells (55). Ag-specific memory T cells differ from the spontaneously occurring memory phenotype T cells in terms of their homeostasis and functionality (9). Therefore, the use of SPF mice for studies on T cell biology might produce data of low relevance in terms of translational value for clinical studies (56). To overcome this limitation, some novel approaches emerged recently, like the use of "dirty mice" (55), which show more relevant immune response in the context of human sepsis (57), nonspecific T cell activation, or combined infections (48). However, in the current study, we aimed to study Ag-experienced memory T cells that reside in the BM. Hence, we designed an experimental protocol of immunization with OVA in mice with adoptively transferred TCR-transgenic, OVA-specific naive $CD4^+$ T cells and subsequently traced the proliferation of these cells after sepsis. By transplantation of naive T cells into nonlymphopenic hosts, we could be certain that before the immunization all OVA-specific T cells were naive and the acquisition of memory markers was induced only upon Ag encounter. Together with the use of sensitive peptide/MHC tetramer staining and population-of-interest enrichment, this protocol allowed us to study the recovery of Ag-specific memory T cells. Consistent with the report by Tokoyoda et al. (30), we found that the majority of Ag-experienced memory T cells migrated to the BM. Although in healthy mice the number of Ag-experienced T cells was higher in the lymph nodes than BM, it should be noted that the analyzed BM was obtained only from 2 femurs because of technical reasons, while its pool is much larger in the whole organism. Our results from experiments using 2 murine background models showed that BM is the preferred site for the proliferation of Ag-specific memory T cells in physiological conditions. Furthermore, the role of BM in sustaining proliferation of $CD4^+$ T cells was more evident in the postseptic mice, which presented an extremely high percentage of proliferating $CD4^+$ T cells. This finding fills an important gap in the knowledge on the role of BM in the homeostasis of the Ag-experienced memory $CD4^+$ T cells (31, 58). Moreover, we observed that at the later time point after sepsis, most of the memory $CD4^+$ T cells that had proliferated at the early time point could be found in the SLOs. Interestingly, the BM $CD4^+$ T cells were separated from the circulating blood because they were not stained by i.v. antibody, which implies that their emigration into circulation must be a coordinated process that requires further investigations. These results are in line with some previous reports suggesting that BM serves as a temporary niche supporting proliferation of recirculating T cells (59, 60). It should be emphasized

that the abovementioned studies were focused on $CD8^+$ T cells, and there has been a pending gap on the role of BM in $CD4^+$ T cells' homeostasis. Lack of in vivo staining and high CD69 expression on the BM $CD4^+$ T cells stays in line with a recent report indicating signature transcripts of Trm cells (61). Taken together our data support a model for BM as a niche for memory $CD4^+$ T cells that fosters their proliferation and allows partial recirculation via blood to other sites (31).

Our data confirm the previously shown specificity of T cells that have predilection for BM homing (30, 62). We further expand this observation by showing that sepsis reduces the capacity of the BM niche for T cells but does not diminish their specific homing capacities. It was a surprising finding because the T cell homing to BM was shown to be a competitive process (62) and at the time of transfer there was a reduced number of endogenous BM $CD4^+$ T cells. Hence, we hypothesized that the decreased capacity of BM for T cells might be related to altered IL-7 availability because BM $CD4^+$ T cells are found in the proximity of IL-7^+ cells (30). Indeed, we observed a massive reduction of IL-7 concentration in the BM. Still, this amount of IL-7 was sufficient to induce proliferation of the BM $CD4^+$ T cells. We cannot exclude the potential role of other molecules contributing to this effect, such as IL-15, OX40, or CD30 (63), yet our results with IL-7 receptor–neutralizing antibodies point at IL-7 as the major regulator of BM $CD4^+$ T cells' proliferation. Importantly, we showed that treatment of septic mice with exogenous rm-IL-7 stimulates proliferation of the BM memory $CD4^+$ T cells, indicating potential clinical utility of IL-7.

Our study has several limitations. All experiments were performed on young male mice to avoid the effects of fluctuating sex hormones on the proliferation of T cells. The applied model is characterized by low mortality, and more severe sepsis may influence the dynamics of T cell recovery. We used TCR-transgenic, OVA-specific $CD4^+$ T cells to study homing and proliferation of Ag-experienced memory T cells. This tool enabled us to transfer naive $CD4^+$ T cells and ensure that acquisition of CD44 marker occurred upon Ag encounter but not homeostatic proliferation. Simple immunization experiments would not allow us to exclude Ag-specific, memory phenotype $CD4^+$ T cells. However, it would be of great interest to verify the role of BM and IL-7 treatment in the maintenance of memory T cells specific for pathogens commonly infecting patients with sepsis, such as *Pseudomonas aeruginosa*, *Staphylococcus aureus*, *Escherichia coli*, or reactivating viruses (cytomegalovirus, Epstein-Barr virus) (64, 65). A recent study on human BM by Okhrimenko et al. (29) revealed that in comparison with peripheral blood, BM is enriched in viral Ag-specific memory $CD4^+$ T cells, while such enrichment was not observed for *Candida albicans*–specific T cells. Also, i.v. immunization of mice with *Listeria monocytogenes* generated a long-term memory $CD4^+$ T cell population in the BM (66). Altogether, we propose that BM is the preferential settlement and proliferation site for the memory $CD4^+$ T cells that responded to systemic Ag challenge. Whether it is also a proliferation site for other memory $CD4^+$ T cells remains to be investigated. Finally, the degree to which the TCR repertoire of memory $CD4^+$ T cells recovers should also be tested in future studies.

In conclusion, we have shown that BM is a principal niche supporting the proliferation of $CD4^+$ Tem cells during recovery from sepsis-induced lymphopenia and under steady-state conditions. These cells are BM resident and require IL-7 for their proliferation. Unraveling this process expands our understanding of the recovery of adaptive immunity in sepsis survivors. Based on our findings we propose that future therapies aimed at boosting T cell recovery should target the BM as the relevant anatomical localization of memory T cell proliferation.

Methods

Mice. All animal experiments were approved by the II Local Ethic Committee and were performed according to Polish and European Union regulations. Male 10- to 12-week-old BALB/c and C57BL/6 mice were obtained from the Mossakowski Medical Research Centre, Polish Academy of Science, Warsaw, Poland, and housed for 7 days before start of the experiments. Mice were housed in the animal facility of the Centre of Postgraduate Medical Education with 12-hour light/12-hour dark cycle and fed with standard sterile food and water ad libitum. OT-II mice [B6.Cg-Tg(TcraTcrb)425Cbn/J] (The Jackson Laboratory) were bred at the Medical University of Warsaw. DO11.10 mice (The Jackson Laboratory) were a gift from Stefanie Flohe from the Essen University Hospital, Essen, Germany.

CLP sepsis. Peritonitis-derived sepsis was modeled by performing the CLP surgery (32) according to the Minimum Quality Threshold in Pre-Clinical Sepsis Studies recommendations (67). All mice received buprenorphine (0.05 mg/kg in 0.1 mL of 0.9% saline i.p.) 20 minutes before surgery. Then, mice were anesthetized with isoflurane. The abdomen was shaved and disinfected with ethanol. After midline laparot-

omy, the cecum was exposed, ligated at half of its length, and punctured twice with a 25-gauge needle to extrude a small amount of cecal content. After repositioning of the cecum, the abdomen was closed with single button sutures (5/0) and Histoacryl tissue adhesive (Aesculap, B. Braun). From 2 hours post-CLP on, all mice received subcutaneous wide-range antibiotic therapy (25 mg/kg imipenem, Zienam; MSD) and fluid resuscitation (1 mL Ringer's solution) with analgesia (0.05 mg/kg buprenorphine, Bupaq; Richter Pharma) twice daily (approximately every 12 hours) for 5 consecutive days after CLP. This model was scaled to result in 30-day mortality not exceeding 10%. For tissue collection mice were sacrificed by cervical dislocation under isoflurane anesthesia. BM was collected by flushing femurs and tibias with 5 mL of PBS. Popliteal and axillary lymph nodes and spleen were cut out for analyses.

Blood lymphocyte count. Changes in the blood lymphocyte counts were analyzed by sampling from living animals. To obtain serial blood samples, 20 μL of blood was taken via facial vein puncture (23-gauge needle) according to a published protocol (68). Blood was diluted in PBS with EDTA and placed in Trucount tubes (BD). Then a mixture of anti–CD3-FITC (17A2, BD) anti–CD4-APC (RM4-4, BioLegend), and anti–CD8a-PE (53-6.7, BioLegend) antibodies was added for 20 minutes' incubation. Erythrocytes were lysed by adding 2 mL of ACK buffer (Thermo Fisher Scientific), and cells were analyzed using FACSCanto II flow cytometer with FACSDiva software (BD).

BrdU in vivo assay. For the analysis of in vivo T cell proliferation, mice were injected i.p. with a single bolus of BrdU (1 mg BrdU in 100 μL 0.9% NaCl; Thermo Fisher Scientific) on a given day after surgery. If not indicated otherwise, 24 hours later, mice were sacrificed, and the retrieved cells were purified from erythrocytes by lysis with ACK buffer. Cells were surface stained with anti–CD4-APC (RM4-4), anti–CD44-PE-Cy7 (IM7), anti–CD62L-biotin (MEL-14) (BioLegend), and streptavidin-APC-Cy7 (BD) followed by permeabilization and DNAse treatment according to the manufacturer's instructions (BrdU FITC Staining Kit, Thermo Fisher Scientific). Finally, cells were stained with FITC anti-BrdU antibody (Bu20a, BrdU FITC Staining Kit, Thermo Fisher Scientific) and analyzed by flow cytometry. In another experiment, cells were stained with anti–CD69-FITC (H1.2F3, BioLegend). In some experiments, septic mice were treated with anti–mouse CD127 antibody (IL-7Rα, Bio X Cell), 0.5 mg/mouse i.p., on days 5 and 6 after CLP and given BrdU bolus i.p. on day 6. In another experiment, septic mice were injected s.c. with a complex of 2.5 μg rm-IL-7 (PeproTech) and 12.5 μg anti–IL-7 (M25, Bio X Cell) in 100 μL of PBS (69) on days 4 and 5 and then were given BrdU pulse on day 6.

Adoptive transfer and immunization. For adoptive transfer experiments, T cells were obtained from BM or spleen of healthy or post-CLP mice. After erythrocyte lysis, cells were stained with anti–CD3-PE (17A2, BD) antibody and CellTrace Violet fluorescent dye (Thermo Fisher Scientific) for 20 minutes at 37°C and washed with 10% fetal calf serum in RPMI 1640 (Thermo Fisher Scientific). Then, cells were resuspended in FACS Wash Buffer (BD), and $CD3^+$ cells were sorted using FACSAria cell sorter (BD). The purity of cells was more than 98%. Purified cells were suspended in 100 μL of 0.9% NaCl, and 5×10^5 cells were injected i.v. into healthy or post-CLP mice. For TCR-specific experiments cells from spleen and lymph nodes of the OT-II male mice were harvested, and $CD4^+$ T cells were isolated using EasySep magnetic separation system (STEMCELL Technologies). Purified cells were stained with anti-CD44 PE-Cy7 antibody (IM7, BioLegend), and negative cells were sorted using FACSAria (BD). Then 1×10^6 $CD4^+CD44^-$ T cells were injected i.v. in 100 μL of saline into C57BL/6 mice. On the next day, mice were injected with 100 μg of OVA (MilliporeSigma) s.c. and 100 μg i.p.

Tetramer staining. Analysis of Ag-specific T cells was performed based on the published tetramer-based protocols (25, 70). Cells harvested from the lymph nodes, BM, and spleens and erythrocytes were lysed with the ACK lysis buffer for 10 minutes on ice. Cells were resuspended in the staining buffer (PBS with 5% fetal bovine serum, 2 mM EDTA, 50 μM dasatinib (Cayman Chemicals), 1:50 heat-inactivated mouse serum, and 1:100 anti-CD16/32 mAb), and the PE-conjugated $I\text{-}A^b$ tetramers were added at 1:100 dilution. $I\text{-}A^b$ chicken $OVA_{329–337}$ (AAHAEINEA) tetramer was used (gift from the NIH Tetramer Core Facility, Atlanta, Georgia, USA). Cells were incubated at 37°C for 1 hour and washed with ice-cold sorting buffer (PBS with 2% FBS and 2 mM EDTA). Then, cells were resuspended in 200 μL of the buffer, and 10 μL of anti-PE nanobeads (BioLegend) was added. The probe was incubated at room temperature for 15 minutes. Afterward, cells were washed 5 times with the sorting buffer. Tetramer-enriched cells were then stained for surface molecules and BrdU as described above. Labeled cells were analyzed and counted using the FACSVerse flow cytometer (BD).

Intravascular staining. Intravascular staining of BM lymphocytes was performed according to the original protocol (36). Six days after CLP mice received i.p. injection of BrdU as described earlier. Then, on

day 7 mice were given an i.v. injection of 3 μg of anti–CD4-APC antibody (RM4-4, BioLegend) in 300 μL of saline. Three minutes after injection mice were killed by cervical dislocation. BM was flushed out of femurs, and the surface and anti-BrdU staining were performed with the following antibodies: anti–CD4-BV421 (RM4-5, BioLegend), anti–CD3-PerCP-eFluor710 (17A2, BioLegend), anti–CD44-Pe-Cy7 (IM7, BioLegend), anti-CD62L biotin (MEL-14, BioLegend), and anti–BrdU-FITC (Bu20a, Thermo Fisher).

Intracellular cytokine staining. Isolated splenocytes and BM cells were stimulated with Cell Activating Cocktail (PMA, ionomycin, and brefeldin A, BioLegend) in RPMI 1640 with 10% FBS (Thermo Fisher Scientific) for 5 hours according to the manufacturer's protocol. Then, cells were stained with anti–CD3-PerCP-eFluor710, anti–CD4-APC, and anti–CD44-Pe-Cy7 antibodies for 20 minutes. Cells were fixed and permeabilized with the Cytofix/Cytoperm buffer set according to the protocol (BD). Intracellular staining was performed with anti–IFN-γ-PE (XMG1), anti–IL-4-PE (11B11), and anti–IL-17A-eFluor450 (17B7) antibodies (all from Thermo Fisher Scientific).

Flow cytometry. Analysis of cell phenotype was performed by incubation of 1×10^6 of the fresh sample's cells with the primary antibodies at room temperature for 20 minutes. Then, cells were washed with PBS containing 2% FBS, and in some cases streptavidin-APC-Cy7 was added for the next 15-minute incubation. After a wash with 2% FBS in PBS, cells were resuspended in 0.5% paraformaldehyde in PBS. Apoptosis was analyzed by incubation of isolated cells with the Vybrant FAM caspase-3/-7 FLICA reagent according to the manufacturer's protocol (Thermo Fisher Scientific). Cells were analyzed using FACSVerse flow cytometer (BD) with FACSDiva software (BD). Analyses were performed with FlowJo software (Tree Star). Appropriate negative and fluorescence minus one controls were used to set gates. T cells were analyzed according to the Minimal Information about T Cell Assays guidelines (71).

Immunofluorescence. Femurs were dissected and cleaned from adherent tissues. Then, bones were placed in the RDC decalcifying buffer (CellPath) for 24 hours and washed under running water. Bones were embedded in paraffin blocks and cut with a microtome. Paraffin was removed by washing in Neoclear solution (MilliporeSigma). Antigen retrieval was performed by heating the slides with EnVision Flex High pH Retrieval Solution (Agilent) in a steamer for 20 minutes. Then, slides were stained overnight at 4°C with 1:100 diluted antibodies in 3% BSA: anti–CD4-eFluor660 (4SM95, Thermo Fisher Scientific), anti–CD44–Alexa Fluor 488 (IM7, Thermo Fisher Scientific), and goat anti–IL-7 (R&D Systems, Bio-Techne). Secondary staining was performed with goat anti-rabbit Alexa Fluor 594 antibody (Thermo Fisher Scientific) diluted 1:200. Stained samples were mounted with Cytomation Fluorescent Mounting Medium (Dako Cytomation). Slides were analyzed under the Axio Observer confocal microscope equipped with ×60 lens (Carl Zeiss) and ZEN software. The same image acquisition and postacquisition settings were applied to all samples. Controls incubated with the secondary antibody were performed secondary antibodies only.

IL-7 measurement. Blood was collected from retro-orbital venous plexus under isoflurane anesthesia. Femurs were flushed with 0.5 mL of PBS and centrifuged. Samples were stored at –80°C. IL-7 concentration was measured using a commercially available ELISA kit (Thermo Fisher Scientific).

Statistics. The results were analyzed using GraphPad Prism 7 software. Normality of data was assessed using Shapiro-Wilk and Kolmogorov-Smirnov normality tests. Data are presented as mean ± SD. Comparisons between groups were performed with 2-tailed Student's *t* test. Multiple comparisons were tested using 1-way ANOVA with Tukey's post hoc test. Each experimental group consisted of at least 5 mice, and experiments were repeated at least 2 times. Graphs present mean ± SD values. *P* value below 0.05 was considered significant.

Study approval. All animal experiments were approved by the II Local Ethic Committee, Warsaw, Poland (WAW2/54/2017 and WAW2/56/2016) and were performed according to Polish and European Union regulations. Animal experiments adhered to the Animal Research: Reporting of In Vivo Experiments guidelines (72).

Author contributions

TS designed the study and performed CLP experiments, FACS analyses, adoptive transfers, antibody treatment, data analysis, and manuscript writing; PS analyzed T cell populations, incorporated BrdU, and corrected the manuscript; GH designed the study and performed CLP experiments, ELISA, tissue section staining, and manuscript correction; JG designed transfer experiments, isolated T cells, and corrected the manuscript; DN designed transfer experiments, isolated T cells, and corrected the manuscript; and EK designed the study, supervised PS, performed FACS and cell sorting, and performed manuscript correction.

Acknowledgments

The authors would like to thank Edyta Brzóska-Wójtowicz from the Department of Cytology, University of Warsaw, for help in obtaining microphotographs. This work was funded by Poland National Science Centre grant UMO-2016/23/D/NZ6/02554 to TS and UMO-2016/23/B/NZ6/03463 to DN, iONKO (Regionalna Inicjatywa Doskonałości) from the Polish Ministry of Science and Higher Education, and Centre of Postgraduate Medical Education grant 5011492118/19.

Address correspondence to: Tomasz Skirecki, Laboratory of Flow Cytometry, Centre of Postgraduate Medical Education, Marymoncka 99/103, 01-813 Warsaw, Poland. Phone: 0048.22.5693.838; Email: tskirecki@cmkp.edu.pl.

1. Reinhart K, Daniels R, Kissoon N, Machado FR, Schachter RD, Finfer S. Recognizing sepsis as a global health priority – a WHO resolution. *N Engl J Med*. 2017;377(5):414–417.
2. Singer M, et al. The Third International Consensus Definitions for Sepsis and Septic Shock (Sepsis-3). *JAMA*. 2016;315(8):801–810.
3. Stevenson EK, Rubenstein AR, Radin GT, Wiener RS, Walkey AJ. Two decades of mortality trends among patients with severe sepsis: a comparative meta-analysis. *Crit Care Med*. 2014;42(3):625–631.
4. Rhee C, et al. Incidence and trends of sepsis in US hospitals using clinical vs claims data, 2009-2014. *JAMA*. 2017;318(13):1241–1249.
5. Prescott HC, Osterholzer JJ, Langa KM, Angus DC, Iwashyna TJ. Late mortality after sepsis: propensity matched cohort study. *BMJ*. 2016;353:i2375.
6. van der Poll T, van de Veerdonk FL, Scicluna BP, Netea MG. The immunopathology of sepsis and potential therapeutic targets. *Nat Rev Immunol*. 2017;17(7):407–420.
7. Sallusto F, Lenig D, Förster R, Lipp M, Lanzavecchia A. Two subsets of memory T lymphocytes with distinct homing potentials and effector functions. *Nature*. 1999;401(6754):708–712.
8. Szabo PA, Miron M, Farber DL. Location, location, location: tissue resident memory T cells in mice and humans. *Sci Immunol*. 2019;4(34):eaas9673.
9. Surh CD, Sprent J. Homeostasis of naive and memory T cells. *Immunity*. 2008;29(6):848–862.
10. Luckheeram RV, Zhou R, Verma AD, Xia B. $CD4^+$T cells: differentiation and functions. *Clin Dev Immunol*. 2012;2012:925135.
11. Zhu J, Paul WE. CD4 T cells: fates, functions, and faults. *Blood*. 2008;112(5):1557–1569.
12. Hoser GA, Skirecki T, Zlotorowicz M, Zielinska-Borkowska U, Kawiak J. Absolute counts of peripheral blood leukocyte subpopulations in intraabdominal sepsis and pneumonia-derived sepsis: a pilot study. *Folia Histochem Cytobiol*. 2012;50(3):420–426.
13. Chang KC, et al. Multiple triggers of cell death in sepsis: death receptor and mitochondrial-mediated apoptosis. *FASEB J*. 2007;21(3):708–719.
14. Drewry AM, Samra N, Skrupky LP, Fuller BM, Compton SM, Hotchkiss RS. Persistent lymphopenia after diagnosis of sepsis predicts mortality. *Shock*. 2014;42(5):383–391.
15. Chung KP, et al. Severe lymphopenia is associated with elevated plasma interleukin-15 levels and increased mortality during severe sepsis. *Shock*. 2015;43(6):569–575.
16. Bermejo-Martin JF, et al. Lymphopenic community acquired pneumonia (L-CAP), an immunological phenotype associated with higher risk of mortality. *EBioMedicine*. 2017;24:231–236.
17. Unsinger J, et al. IL-7 promotes T cell viability, trafficking, and functionality and improves survival in sepsis. *J Immunol*. 2010;184(7):3768–3779.
18. Inoue S, et al. IL-15 prevents apoptosis, reverses innate and adaptive immune dysfunction, and improves survival in sepsis. *J Immunol*. 2010;184(3):1401–1409.
19. Chang KC, et al. Blockade of the negative co-stimulatory molecules PD-1 and CTLA-4 improves survival in primary and secondary fungal sepsis. *Crit Care*. 2013;17(3):R85.
20. Hotchkiss RS, et al. Prevention of lymphocyte cell death in sepsis improves survival in mice. *Proc Natl Acad Sci U S A*. 1999;96(25):14541–14546.
21. Francois B, et al. Interleukin-7 restores lymphocytes in septic shock: the IRIS-7 randomized clinical trial. *JCI Insight*. 2018;3(5):98960.
22. Rubio I, et al. Current gaps in sepsis immunology: new opportunities for translational research. *Lancet Infect Dis*. 2019;19(12):e422–e436.
23. Venet F, et al. Decreased T-cell repertoire diversity in sepsis: a preliminary study. *Crit Care Med*. 2013;41(1):111–119.
24. Unsinger J, Kazama H, McDonough JS, Hotchkiss RS, Ferguson TA. Differential lymphopenia-induced homeostatic proliferation for CD4+ and CD8+ T cells following septic injury. *J Leukoc Biol*. 2009;85(3):382–390.
25. Cabrera-Perez J, et al. Alterations in antigen-specific naive CD4 T cell precursors after sepsis impairs their responsiveness to pathogen challenge. *J Immunol*. 2015;194(4):1609–1620.
26. Condotta SA, Rai D, James BR, Griffith TS, Badovinac VP. Sustained and incomplete recovery of naive CD8+ T cell precursors after sepsis contributes to impaired CD8+ T cell responses to infection. *J Immunol*. 2013;190(5):1991–2000.
27. Ammer-Herrmenau C, et al. Sepsis induces long-lasting impairments in CD4+ T-cell responses despite rapid numerical recovery of T-lymphocyte populations. *PLoS ONE*. 2019;14(2):e0211716.
28. Herndler-Brandstetter D, et al. Human bone marrow hosts polyfunctional memory CD4+ and CD8+ T cells with close contact to IL-15-producing cells. *J Immunol*. 2011;186(12):6965–6971.
29. Okhrimenko A, et al. Human memory T cells from the bone marrow are resting and maintain long-lasting systemic memory.

Proc Natl Acad Sci U S A. 2014;111(25):9229–9234.
30. Tokoyoda K, et al. Professional memory CD4+ T lymphocytes preferentially reside and rest in the bone marrow. *Immunity*. 2009;30(5):721–730.
31. Di Rosa F. Two niches in the bone marrow: a hypothesis on life-long T cell memory. *Trends Immunol*. 2016;37(8):503–512.
32. Wichterman KA, Baue AE, Chaudry IH. Sepsis and septic shock--a review of laboratory models and a proposal. *J Surg Res*. 1980;29(2):189–201.
33. Boyman O, Létourneau S, Krieg C, Sprent J. Homeostatic proliferation and survival of naïve and memory T cells. *Eur J Immunol*. 2009;39(8):2088–2094.
34. Shinoda K, et al. Type II membrane protein CD69 regulates the formation of resting T-helper memory. *Proc Natl Acad Sci U S A*. 2012;109(19):7409–7414.
35. Schmoeckel K, Traffehn S, Eger C, Pötschke C, Bröker BM. Full activation of CD4+ T cells early during sepsis requires specific antigen. *Shock*. 2015;43(2):192–200.
36. Anderson KG, et al. Intravascular staining for discrimination of vascular and tissue leukocytes. *Nat Protoc*. 2014;9(1):209–222.
37. Matiašová A, Sevc J, Mikeš J, Jendželovský R, Daxnerová Z, Fedoročko P. Flow cytometric determination of 5-bromo-2'-deoxyuridine pharmacokinetics in blood serum after intraperitoneal administration to rats and mice. *Histochem Cell Biol*. 2014;142(6):703–712.
38. Mohri H, Bonhoeffer S, Monard S, Perelson AS, Ho DD. Rapid turnover of T lymphocytes in SIV-infected rhesus macaques. *Science*. 1998;279(5354):1223–1227.
39. Ganusov VV, De Boer RJ. A mechanistic model for bromodeoxyuridine dilution naturally explains labelling data of self-renewing T cell populations. *J R Soc Interface*. 2013;10(78):20120617.
40. Westera L, et al. Closing the gap between T-cell life span estimates from stable isotope-labeling studies in mice and humans. *Blood*. 2013;122(13):2205–2212.
41. Venet F, et al. IL-7 restores lymphocyte functions in septic patients. *J Immunol*. 2012;189(10):5073–5081.
42. Andreu-Ballester JC, et al. Deficit of interleukin 7 in septic patients. *Int Immunopharmacol*. 2014;23(1):73–76.
43. Prescott HC, Angus DC. Enhancing recovery from sepsis: a review. *JAMA*. 2018;319(1):62–75.
44. den Braber I, et al. Maintenance of peripheral naive T cells is sustained by thymus output in mice but not humans. *Immunity*. 2012;36(2):288–297.
45. Gabor MJ, Scollay R, Godfrey DI. Thymic T cell export is not influenced by the peripheral T cell pool. *Eur J Immunol*. 1997;27(11):2986–2993.
46. Kong Y, et al. Sepsis-induced thymic atrophy is associated with defects in early lymphopoiesis. *Stem Cells*. 2016;34(12):2902–2915.
47. Terashima A, Okamoto K, Nakashima T, Akira S, Ikuta K, Takayanagi H. Sepsis-induced osteoblast ablation causes immunodeficiency. *Immunity*. 2016;44(6):1434–1443.
48. Xie J, et al. Increased attrition of memory T cells during sepsis requires 2B4. *JCI Insight*. 2019;4(9):126030.
49. Paiardini M, et al. Bone marrow-based homeostatic proliferation of mature T cells in nonhuman primates: implications for AIDS pathogenesis. *Blood*. 2009;113(3):612–621.
50. Skirecki T, et al. Mobilization of stem and progenitor cells in septic shock patients. *Sci Rep*. 2019;9(1):3289.
51. Feuerer M, et al. Bone marrow as a priming site for T-cell responses to blood-borne antigen. *Nat Med*. 2003;9(9):1151–1157.
52. Saule P, Trauet J, Dutriez V, Lekeux V, Dessaint JP, Labalette M. Accumulation of memory T cells from childhood to old age: central and effector memory cells in CD4(+) versus effector memory and terminally differentiated memory cells in CD8(+) compartment. *Mech Ageing Dev*. 2006;127(3):274–281.
53. Thome JJ, et al. Spatial map of human T cell compartmentalization and maintenance over decades of life. *Cell*. 2014;159(4):814–828.
54. Sprent J, Surh CD. Normal T cell homeostasis: the conversion of naive cells into memory-phenotype cells. *Nat Immunol*. 2011;12(6):478–484.
55. Beura LK, et al. Normalizing the environment recapitulates adult human immune traits in laboratory mice. *Nature*. 2016;532(7600):512–516.
56. Stortz JA, Raymond SL, Mira JC, Moldawer LL, Mohr AM, Efron PA. Murine models of sepsis and trauma: can we bridge the gap? *ILAR J*. 2017;58(1):90–105.
57. Huggins MA, et al. Microbial exposure enhances immunity to pathogens recognized by TLR2 but increases susceptibility to cytokine storm through TLR4 sensitization. *Cell Rep*. 2019;28(7):1729–1743.e5.
58. Chang HD, Tokoyoda K, Radbruch A. Immunological memories of the bone marrow. *Immunol Rev*. 2018;283(1):86–98.
59. Di Rosa F, Gebhardt T. Bone marrow T cells and the integrated functions of recirculating and tissue-resident memory T cells. *Front Immunol*. 2016;7:51.
60. Klonowski KD, Williams KJ, Marzo AL, Blair DA, Lingenheld EG, Lefrançois L. Dynamics of blood-borne CD8 memory T cell migration in vivo. *Immunity*. 2004;20(5):551–562.
61. Siracusa F, et al. $CD69^+$ memory T lymphocytes of the bone marrow and spleen express the signature transcripts of tissue-resident memory T lymphocytes. *Eur J Immunol*. 2019;49(6):966–968.
62. Di Rosa F, Santoni A. Memory T-cell competition for bone marrow seeding. *Immunology*. 2003;108(3):296–304.
63. Sabbagh L, Snell LM, Watts TH. TNF family ligands define niches for T cell memory. *Trends Immunol*. 2007;28(8):333–339.
64. Walton AH, et al. Reactivation of multiple viruses in patients with sepsis. *PLoS One*. 2014;9(2):e98819.
65. Wang T, Derhovanessian A, De Cruz S, Belperio JA, Deng JC, Hoo GS. Subsequent infections in survivors of sepsis: epidemiology and outcomes. *J Intensive Care Med*. 2014;29(2):87–95.
66. Pepper M, et al. Different routes of bacterial infection induce long-lived TH1 memory cells and short-lived TH17 cells. *Nat Immunol*. 2010;11(1):83–89.
67. Osuchowski MF, et al. Minimum Quality Threshold in Pre-Clinical Sepsis Studies (MQTiPSS): an international expert consensus initiative for improvement of animal modeling in sepsis. *Infection*. 2018;46(5):687–691.
68. Weixelbaumer KM, Raeven P, Redl H, van Griensven M, Bahrami S, Osuchowski MF. Repetitive low-volume blood sampling

method as a feasible monitoring tool in a mouse model of sepsis. *Shock*. 2010;34(4):420–426.
69. Boyman O, Ramsey C, Kim DM, Sprent J, Surh CD. IL-7/anti-IL-7 mAb complexes restore T cell development and induce homeostatic T cell expansion without lymphopenia. *J Immunol*. 2008;180(11):7265–7275.
70. Moon JJ, et al. Naive CD4(+) T cell frequency varies for different epitopes and predicts repertoire diversity and response magnitude. *Immunity*. 2007;27(2):203–213.
71. Britten CM, et al. T cell assays and MIATA: the essential minimum for maximum impact. *Immunity*. 2012;37(1):1–2.
72. Kilkenny C, Browne W, Cuthill IC, Emerson M, Altman DG, National Centre for the Replacement, Refinement Reduction of Amimals in Research. Animal research: reporting in vivo experiments--the ARRIVE guidelines. *J Cereb Blood Flow Metab*. 2011;31(4):991–993.